A Phenomenological Description of Electron Paramagnetic Double-Resonance Relaxation of Organic Free Radicals in Solution. II. ENDOR Relaxation of Galvinoxyl

Hideo SHIKATA and Kazuhiko ISHIZU*

Laboratory of Chemistry, Faculty of General Education, Ehime University, Bunkyo-cho, Matsuyama 790
**Department of Chemistry, Faculty of Science, Ehime University, Bunkyo-cho, Matsuyama 790*

(Received September 6, 1976)

The ratio of the ENDOR enhancement to the ESR intensity (E) of galvinoxyl in toluene was measured under various conditions of microwave power, rf power and temperature. The results are discussed in comparison with a phenomenological theory in part I. It is proven that the apparent longitudinal electron spin relaxation time for a *t*-butyl proton under NMR excitation is about twice as long as those for methylidyne and ring protons, which is explained by the effect of incomplete hf separation. Also, it is shown that the reciprocal of the slope of the plot of E^{-1} *vs.* (rf power)$^{-1}$ for methylidyne and ring protons is approximately proportional to the number of equivalent protons, whereas that for a *t*-butyl proton can be explained only if the effect of incomplete hf separation is taken into consideration. The value of $b=W_n/W_e$ for methylidyne and ring protons, simulated from the temperature dependence of E based on a previous theory, can be closely correlated to the spin distribution in galvinoxyl.

A phenomenological theory has been described in part I. The purpose of the present paper is to report the results of an experimental examination of the applicability and the limits of the theory.

Because the pulse technique[1,2] is not widespread in the field of ESR spectroscopy, experimental information about the relaxational behavior of a radical can usually be extracted from an analysis of the ESR saturation curve, as well as from that of the linewidth.[3] The same procedure should be applied to ENDOR, by measuring the microwave(mw)- and rf-power dependence of ENDOR enhancement. More abundant information is expected from ENDOR, because two parameters can be varied independently. Recently, Leniart *et al.*[4] have applied such a method to the study of some semiquinones. However, to the present authors' knowledge, there has been no attempt to compare this dependence for different proton species in a molecule over a wide temperature range.

In the present study, the ratio of the ENDOR enhancement to the ESR intensity was measured for different protons, as functions of the mw and rf powers at temperatures from −20 to −95 °C. The sample used in the experiments is the galvinoxyl radical which has one methylidyne proton, four ring protons and thirty-six *t*-butyl protons. It was selected because its ENDOR spectra is one of the most easily observable and because the purity of this very stable radical can be precisely determined from a measurement of the magnetic susceptibility, so that a solution of known concentration can be easily obtained. It is one of materials for which the liquid phase ENDOR was first successfully observed.[5] The results are discussed with reference to the theory in part I, forcussing our attention on a comparison of the proton species.

Experimental

The ENDOR spectra were measured using a JEOL EDX-1 ENDOR unit with a frequency modulation of 6.5 kHz, attached to a JEOL ME-X ESR spectrometer with a field modulation of 80 Hz. The rf amplifier employed can provide maximum rf power of 1 kW. The mw power was calibrated using the ESR intensity of a powdered DPPH radical. The rf power was measured using a level meter connected to a tunk circuit which was calibrated by a 100-MHz oscilloscope, using a search coil. No attempt was made to determine the absolute value of either magnetic field. The intensity of the 80-Hz field modulation was set to a value 3 db lower than that for optimum ENDOR enhancement, because overmodulation reduces the relative enhancement for a *t*-butyl proton with respect the enhancement of other protons.[6]

A toluene solution of galvinoxyl in a quartz tube was degassed using the usual method. The purity of the compound synthesized in this laboratory in the past has been determined to be 85%. The viscosity of toluene was estimated using the empirical formula reported by Barlow *et al.*[7] In most of cases, the ENDOR enhancement was observed at concentration a little more dilute than optimum. The ESR and ENDOR intensity were measured as the peak-to-peak heights of the first derivatives of lines. However, because the ENDOR enhancement for the *t*-butyl proton was not resolved completely at high temperatures, it was measured as the distance from the highest to the lowest peak of the doublet enhancement.

Results and Discussion

An example of an ESR spectrum and an ENDOR spectrum of galvinoxyl (Fig. 1) at −80 °C are shown in Fig. 2. For the latter measurement, the ESR field was adjusted to the highest peak of the low-field part of the doublet of the methylidyne proton. The ESR spectrum completely splits the doublet of quintets of methylidyne and ring protons, but does not resolve any

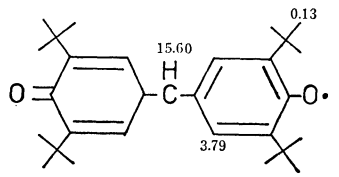

Fig. 1. Structure of galvinoxyl. The numbers indicate the hfs constant in MHz.

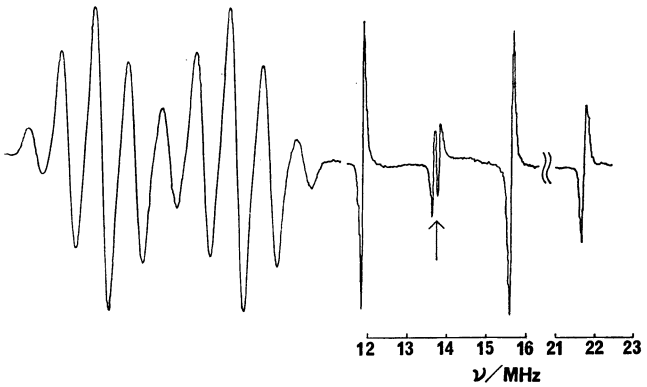

Fig. 2. ESR and ENDOR spectra of galvinoxyl in toluene at −80 °C. The arrow indicates the free proton frequency.

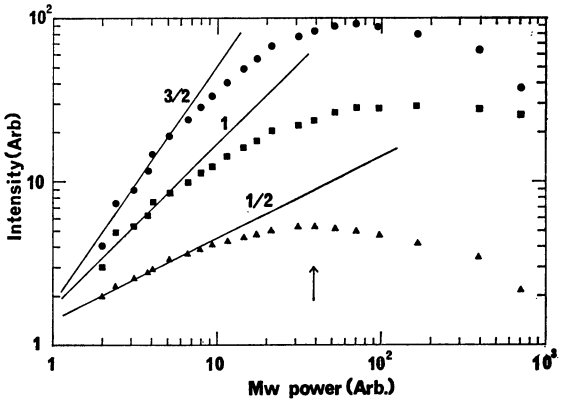

Fig. 3. Dependence of ESR intensity I_{ESR} (▲), ENDOR enhancement I_{ENDOR} (●) and ENDOR quotient I_{ENDOR}/I_{ESR} (■) of ring protons on mw power. The arrow indicates the mw power used for the measurement in Figs. 5—8. The numbers on the lines indicate the order in the low mw-power region.

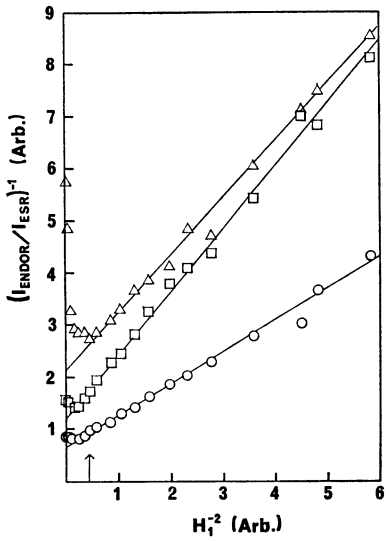

Fig. 4. Reciprocal of the ENDOR quotient as a function of the reciprocal of the mw power. The triangles are for *t*-butyl protons, circles for ring protons and square for a methylidyne proton. The arrow indicates the same mw power as in Fig. 3.

t-butyl proton splitting. From the ENDOR spectrum, however, the hfs constants are found to be 15.60, 3.79, and 0.13 MHz at −80 °C, corresponding to methylidyne, ring and *t*-butyl protons, respectively. No marked dependence of the hfs constants on temperature was observed. In the following discussion, the proton species in galvinoxyl are denoted by the subscripts, m, r, and tb, respectively.

In the present work, the ENDOR enhancement is always divided by the ESR intensity of the peak for which the ENDOR was observed. The quantity, which we tentatively call the ENDOR quotient, is taken to be proportional to the fractional ENDOR enhancement. This procedure will remove experimental errors which may result from, for example, a change in Q value of the cavity during the measurement of the mw-power, rf-power and the temperature dependence. Moreover, the ENDOR quotient is more favorable from the viewpoint of theoretical analysis.

Regarding variation of concentration, the ENDOR enhancement is optimized at about 3×10^{-4} M, and is sharply decreased for other concentrations. On the other hand, as the concentration decreases, the ENDOR quotient monotonically increases and appears to approach to a limiting value. More detailed results will be discussed in a subsequent paper, and it is merely noted that the ratio of the ENDOR enhancement for different protons at the concentration used here is almost the same as the limiting ratio. Thus, we temporarily neglect the Heisenberg exchange effect, as well as the chemical exchange effect, because the addition of another ambiguous parameter would not aid in understanding the essential features of the present system.

(a) Dependence on mw Power. Figure 3 shows the dependence of the ESR intensity, the ENDOR enhancement and the ENDOR quotient on the mw power, measured for ring protons at −75 °C. The rf power employed is indicated by the arrowed in Fig. 5. This figure shows that for sufficiently weak mw powers, the ESR intensity is proportional to the square root of the mw power, the ENDOR enhancement to the 3/2 power of the mw power, so that the ENDOR quotient is proportional simply to the mw power, as is predicted by Eqs. 23—25 in part I. Also, interesting features are found in Fig. 4, in which the reciprocal of the ENDOR quotient for different protons is plotted against the reciprocal of the mw power. As the mw power is increased over a moderately wide range, all the plots go down linearly, but they start to turn up as the mw power is further increased. This means that the ENDOR enhancement decreases more rapidly than does the ESR intensity with a further increase of the mw power. Such a tendency is most marked for *t*-butyl protons, and a more detailed examination reveals that the mw power corresponding to the point at which the plot deviates from a straight line for this proton is about one-half of those for methylidyne and ring protons.

From the theory of part I, the effect of incomplete hf separation is parametrized by a coefficient, α, defined by

$$\alpha = \frac{1}{1+T_{2e}^2\Delta\omega^2}, \quad (1)$$

where $\Delta\omega$ is the hfs constant. Considering that the ESR resolves no splitting for *t*-butyl protons in contrast to the case for methylidyne and ring protons and that T_{2e} ordinarily has a value of 10^{-6}—10^{-7} s, the α for galvinoxyl will be $0 \lesssim \alpha_m$ and $\alpha_r \ll \alpha_{tb} \lesssim 1$. It was shown in part I that the plot of E^{-1} *vs.* p_e^{-1} forms a straight line in the weak mw-power region and that the deviation from linearity at higher mw powers is due to the quadratic terms for p_e, which are proportional to α (Eq. 32 in part I). Thus, the theory explains well the experimental features mentioned above taking account of the difference in the α values.

Furthermore, the effective longitudinal electron spin relaxation time, T_{1e}, under rf-power excitation is given by Eq. 34 in part I. Since $b \ll 1$ at temperatures normally used for ENDOR (as shown in (*c*)), this equation is reduced to

$$T_{1e} \simeq \begin{cases} \dfrac{1}{2W_e} & (\alpha=0) \\ \dfrac{1}{W_e} & (\alpha=1). \end{cases} \quad (2)$$

On the other hand, the slope divided by the intercept of the linear part of the plot in Fig. 4 is interpreted as being proportional to $T_{1e}T_{2e}$. The experimental ratio was 1 : 1.0 : 1.9 for methylidyne, ring and *t*-butyl protons, respectively. The good agreement between the experimental and theoretical results suggests the validity of the treatment for the effect of incomplete hf separation given in part I, although coherence effects[8] may also be involved in the upward-turning tendency of the curve in the high mw-power region in Fig. 4. This is beyond of the limits of the theory in part I.

A similar situation for the mw-power saturation of ENDOR enhancement is also found for the 2,4,6-tri-*t*-butylphenoxyl radical in mineral oil,[6] where the values of the mw power for optimum ENDOR enhancement decreases in the order, 2,6-di-*t*-butyl, 4-*t*-butyl and 3,5-ring protons. Such a result suggests the importance of the effect of incomplete hf separation for the former two types of protons.

(b) Dependence on rf Power. During the analysis of ENDOR enhancement as a function of rf power, the effect of hf enhancement must be kept in mind.[9] In addition to the external rf field, the nuclear spin is affected by another field, caused by the rf modulation of the hf coupling with the electron spin, so that if $|\Delta\omega|/2 < \omega_p$, the effective rf field is given by

$$H_{2eff} = \left(1 \pm \frac{|\Delta\omega|}{2\omega_p}\right) H_2 = \frac{\omega_{n0}}{\omega_p} H_2, \quad (3)$$

where the plus and minus signs correspond to the high- and low-frequency ENDOR lines, respectively, and ω_p is the free proton frequency. However, since the rf power is usually monitored by a search coil having an ω-dependent induced voltage $V = -\partial\Phi/\partial t \propto \omega_{n0}H_2$, no correction was made for this effect in the present work.

Figure 5 shows the rf-power dependence of the high-frequency ENDOR lines measured for different protons at −80 °C, using the values of the mw power indicated by arrows in Figs. 3 and 4. Figure 6, which shows a reciprocal plot of Fig. 5, indicates that the data fall well along a straight line.[10] Equation 28 in part I predicts this linearity. Also, this equation indicates that the linewidth of the ENDOR enhancement increases as the rf power increases, which agrees with what is found experimentally. On the other hand, it is found that this linewidth decreases with temperature. This is qualitatively explained using the same equation, considering that the T_{2n} of a radical is mainly composed of W_e (see Eq. 9).

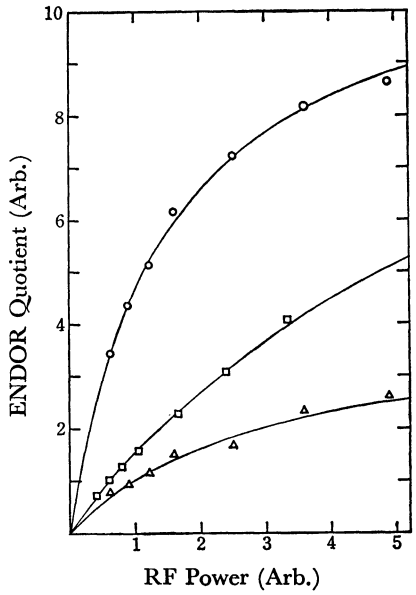

Fig. 5. ENDOR quotient as a function of rf power. The arrow indicates the rf power used for measurements of Figs. 3 and 4.

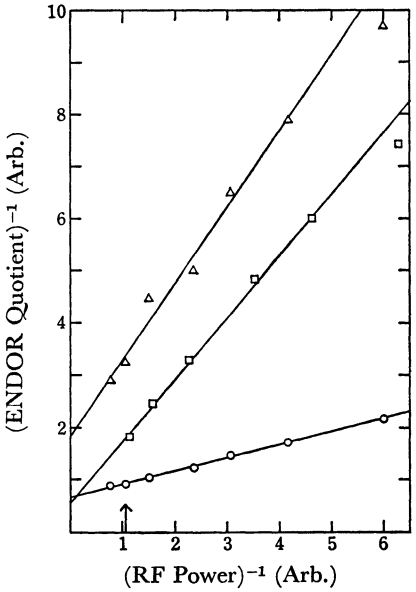

Fig. 6. Reciprocal of the ENDOR quotient as a fuction of the reciprocal of the rf power. The triangles are for *t*-butyl protons, circles for ring protons and squares for a methylidyne proton.

(c) Dependence on Temperature. The ENDOR enhancement is known to vary with temperature in a

rather interesting fashion: it sharply increases to a maximum at a specific value of the ratio of the viscosity to the temperature, $(\eta/T)_{opt}$, independent of the kind of solvent.[11] $(\eta/T)_{opt}$ increases as the size of the molecule decreases[12] and as the spin density on the carbon atom, to which an observed proton is bonded, decreases.[11,12] All this appears to be due to the fact that the fractional ENDOR enhancement is maximum at the temperature for which $b=W_n/W_e$ has a certain value characteristic of the observed proton. Accordingly, from an analysis of the temperature dependence, it should be possible to obtain the ratio of the values of b for different protons in a molecule or even information about its spin distribution. However, because an actual molecule contains several sets of equivalent protons, it is preferable for a quantitative discussion to use a theory for a multi-level system rather than the simple theory for a four-level system. Such a theory was presented in part I and is seen to predict that the ENDOR enhancement is proportional to the number of equivalent protons,[13] if a weak rf power is irradiated with $b \ll 1$ and the effect of incomplete hf separation can be neglected. This has sufficient value for use as an analytical tool such that its applicability should be examined experimentally over the whole temperature range used in ENDOR measurements.

For the above reasons, the ENDOR quotients for different protons in galvinoxyl were measured at temperatures from −20 to −95 °C, by varying the rf power at five points for each temperature. Such measurements and a comparison of the results with theory requires specification of both the mw and rf powers. It was shown in (*a*) that the slope divided by the intercept for a methylidyne proton in the plot in Fig. 4 is identical to that for ring protons. This means the ratio of the ENDOR quotients for both protons at any

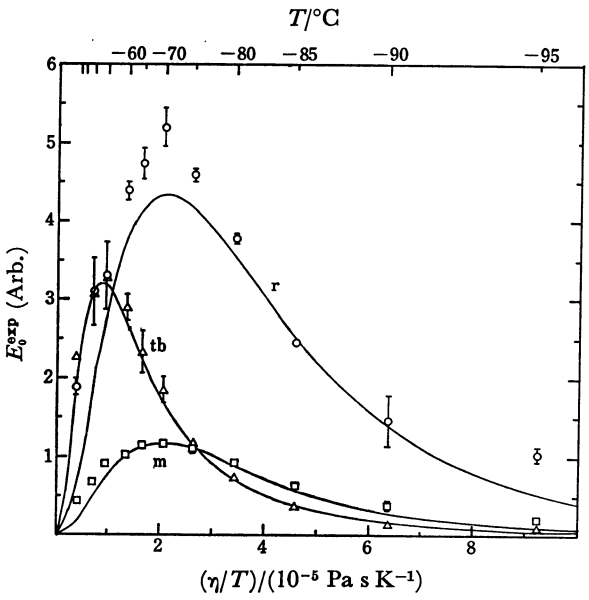

Fig. 7. E_0^{exp} as a function of η/T. The vertical lines indicate the probable error, as determined by the least-squares method. The solid lines are theoretical results. The triangles are for *t*-butyl protons, circles for ring protons and squares for a methylidyne proton.

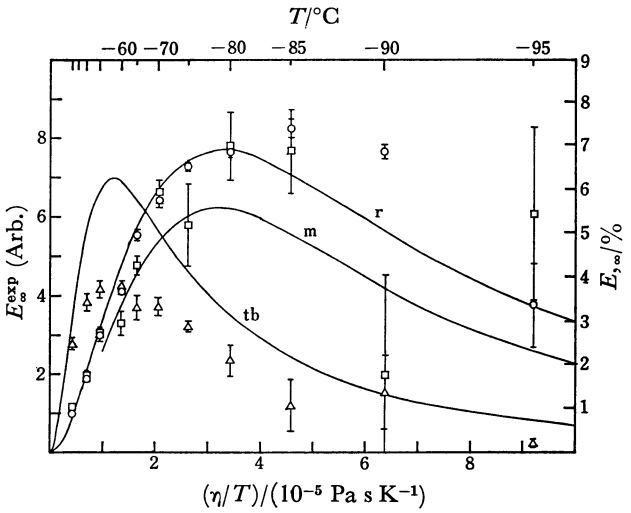

Fig. 8. E_∞^{exp} as a function of η/T. The vertical lines indicate the probable error, as determined by the least-squares method. The solid lines are theoretical results. The triangles are for *t*-butyl protons, circles for ring protons and squares for methylidyne proton.

mw power is identical to that at infinite mw power. The mw power employed in this experiment corresponds to the maximum ESR intensity. Also, the rf power can be specified if the reciprocals of the slope and the intercept are determined from a similar plot shown in Fig. 6, because they correspond to the ENDOR quotients at infinitesimal and infinite rf powers, E_0^{exp} and E_∞^{exp}, respectively. E_0^{exp} and E_∞^{exp} thus determined are shown in Figs. 7 and 8 as a function of η/T. These are analyzed using the following procedure.

Simulation. According to the theory of part I for a multi-level system consisting of several sets of equivalent protons, the fractional ENDOR enhancement at infinitesimal and infinite rf powers are approximately given by Eqs. 50 and 52 and by Eqs. 49 and 51, respectively, with Eqs. 46—48 in part I. The transition probabilities in these equations have been formulated by Freed and Fraenkel[14] and by Freed.[15] Accordingly, if we have information about the g tensor, hf tensor and the other molecular parameters of this radical, we can in principle calculate these values and thus the fractional ENDOR enhancement. Atherton and Day[16] have performed such an estimation for a methylidyne proton in galvinoxyl. However, this involves considerable ambiguities at the present stage. For instance, the rotational correlation time of a molecule, τ_R, is expressed by the extended Debye relationship as

$$\tau_R = \frac{4\pi\kappa r^3\eta}{3kT}. \quad (4)$$

The hydrodynamic radius, r, and a constant, κ, are both dependent on the molecular structures of the radical and the solvent, and consequently, involve unavoidable ambiguities.

For this reason, here, only the η/T dependence of each transition probability is assigned under the following assumptions in an attempt to examine how the fractional ENDOR enhancement varie with temperature. A moderately slow tumbling molecular motion is

assumed so that the following conditions are satisfied:

$$\omega_{e0}^2\tau_R^2 \gg 1, \quad \omega_{n0}^2\tau_R^2 \ll 1. \tag{5}$$

For W_e, we neglect the contribution from the END interaction, as well as the spin rotational interaction, and thus it is assumed to be independent of the nuclear spin quantum numbers. Then, denoting the spectral density by $j(\omega)$, the η/T dependence of the transition probabilities can be written as

$$W_e \approx 2j_{G_s}(\omega_{e0})H_0^2 \approx \frac{1}{\tau_R} \approx \frac{T}{\eta}, \tag{6}$$

and

$$W_n^{(u)} \approx \frac{1}{2}j_D^{(u)}(0) \approx \tau_R \approx \frac{\eta}{T}, \tag{7}$$

so that

$$b_u \approx \frac{j_D^{(u)}(0)}{4j_{G_s}(\omega_{e0})} \approx \tau_R^2 \approx \left(\frac{\eta}{T}\right)^2. \tag{8}$$

Also, the η/T dependence of T_{2n} is derived from

$$\frac{1}{T_{2n}(J_u)} = W_e\left\{1+\left(2f_{J_u}+\frac{1}{3}\right)b_u\right\}. \tag{9}$$

We assume p_e and T_{2e} to have constant values of 1/2 and 1.2 μs, respectively, independent of the temperature. (The choice of the latter value is discussed below.)

If we choose given values of b_m, b_r, and b_{tb} at any temperature and apply these equations to Eqs. 50 and 52 in part I, the relative values of $E_{,0}$ for each proton in galvinoxyl are readily evaluated for all temperatures. Thus, the values of b_m, b_r, and b_{tb} are determined in such a way that the experimental and theoretical T_{opt} for $E_{,0}$ are in complete agreement, since the T_{opt} for $E_{,0}^{exp}$ are known precisely for each proton. Then, using the values of b thus determined, the values of $E_{,\infty}$ are calculated for each proton from Eqs. 49 and 51 in part I. The results are shown by solid lines in Figs. 7 and 8. In Fig. 7, the values of $E_{,0}$ are normalized to that of E_0^{exp} for a methylidyne proton at the optimum temperature for this proton.

Comparison of Experimental and Theoretical Results. Because the determination of the E_0^{exp} involves much smaller errors than that of the E_∞^{exp}, the T_{opt} in Fig. 7 are unambiguously obtained to be −70, −70, and −50 °C for the methylidyne, ring and *t*-butyl protons, respectively. On the other hand, these temperatures are not clear in Fig. 8. However, repeated experiments indicate the T_{opt} to be about −55 °C for the *t*-butyl protons and in the neighborhood of −80——85 °C for the methylidyne and ring protons. Thus, E_0^{exp} has a maximum at a value of η/T of about one-half of that for E_∞^{exp}. In addition, E_0^{exp} decreases more rapidly than does E_∞^{exp} for temperatures below the T_{opt}. The theoretical curves describe these features well. However, at very low temperatures, the theoretical curves tend to be below the experimental points in both figures, as was more evidently confirmed from repeated experiments. This is believed to arise from the $b_u \ll 1$ assumption which is invalid at these temperatures. In Eqs. 49—52 in part I, the relaxation pathways for the END terms of protons other than that observed contribute only to the denominator, so that the fractional ENDOR enhancement tends to be underestimated when $b_u \gtrsim 1$.

Regarding the relative intensity, E_0^{exp} for the methylidyne proton in Fig. 7 is about four times smaller than that for the ring protons. This is more clearly

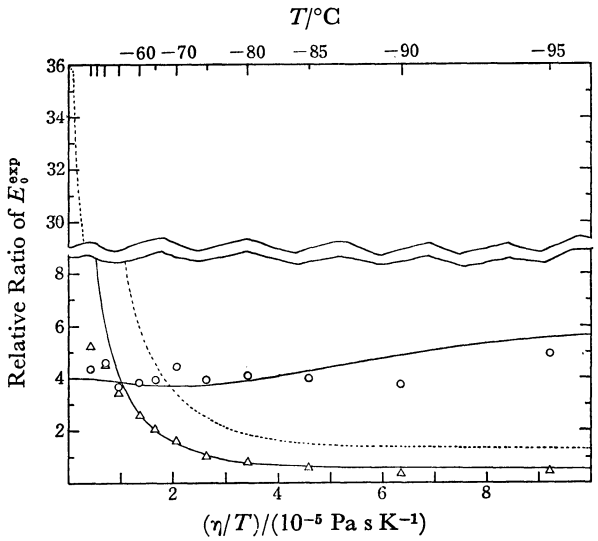

Fig. 9. Ratio of E_0^{exp} values for *t*-butyl protons (△) and ring protons (○) to E_0^{exp} for a methylidyne proton as a function of η/T. The solid lines are theoretical results.

indicated in Fig. 9, in which the ratios of the values of $E_{,0}$ for the ring and *t*-butyl protons to that for the methylidyne proton are plotted against η/T. It is encouraging that the experimental and theoretical values of $E_{,0}$ for the methylidyne and ring protons are approximately proportional to the number of equivalent protons even at temperatures for which the condition, $b_u \ll 1$, is not necessarily valid. On the other hand, in Fig. 8, the E_0^{exp} for a methylidyne proton agrees with that for ring protons (see also Fig. 6), whereas the theoretical counterparts at optimum temperatures, −79 °C (b_m=0.84 and b_r=0.29), are 5.6 and 6.9% for methylidyne and ring protons, respectively, with a ratio of 1.26. The quantitative justification of these values is left until absolute measurements of fractional ENDOR enhancement are performed. However, it should be noted that the calculated values are much smaller than the value, 12.5%, expected from the simple theory for a four-level system.

It is worthwhile to discuss the correlation of the values of b estimated from Fig. 7 with the spin distribution in galvinoxyl. The value of b obtained at −70 °C (η/T= 2.05×10^{-5} Pa s K^{-1}) are b_m=0.32 and b_r=0.11 with b_m/b_r=2.9. Luckhurst[17] has studied in detail the structure and the spin distribution of galvinoxyl, and has found ρ_m=−0.0748 and ρ_r=−0.0448. It is considered that $W_n^{(u)}$ is proportional to the square of the spin density on the carbon atom to which the u'th proton is bonded.[11,18] Thus, the above ratio of b values should be 2.79. The good agreement between both values shows the close correlation between the spin density and the ENDOR relaxation. Also, the agreement seen at high temperatures between the E_∞^{exp} values for the methylidyne and ring protons in Fig. 8 leads to a ratio in the neighborhood of 2, using Eq. 54 in part I.

Now the ENDOR quotient for *t*-butyl protons will be considered. The experimental results show two peculiar features, (1) the high optimum temperature, as seen in both Figs. 7 and 8, in spite of the fact that a

proton with a smaller END term should have a lower optimum temperature, and (2) the much smaller ratio of E_0^{exp} for this proton to that for the methylidyne proton than would be expected from the number of equivalent protons (see Fig. 9).

Such a high optimum temperature for this proton is also found for 2,4,6-tri-*t*-butylphenoxyl,[6] 2,5-di-*t*-butyl-*p*-benzosemiquinone[11] and *m,m,m'm'*-tetra-*t*-butylbiphenyl[12] and appears to be characteristic of *t*-butyl protons. Allendoerfer and Maki[6] have suggested that this is attributable to the effect of incomplete hf separation. Considering only the secular terms for the same assumption under which Eq. 6 is based, T_{2e} may decrease with temperature as follows:

$$\frac{1}{T_{2e}} \approx \frac{8}{3} j_{G_s}(0) H_0^2 \approx \tau_R \approx \frac{\eta}{T}, \quad (10)$$

so that this effect is more prominent at lower temperatures and results in a higher optimum temperature. However, simulation shows that this effect requires a T_{2e} as short as 10 ns at −50 °C in order to produce such a high temperature with the result that the ENDOR enhancement becomes negligibly small. In addition, the apparent ESR linewidth for galvinoxyl was found to decrease with temperature down to −20 °C, is constant as a whole from −20 to −70 °C, and increases rapidly at lower temperatures. This implies that nonsecular and pseudosecular terms, as well as the contribution from the spin-rotational interaction, compete with secular terms in Eq. 10 at high temperatures.

It is believed that the high optimum temperature is attributable rather to the large average total nuclear-spin quantum number of the *t*-butyl protons. Let us assume a crude four-level system for *t*-butyl protons whose relaxation pathways involve only the W_e and the $\langle f_{Ju} \rangle W_n^{(u)}$, the average nulear-spin transition probability, which is given by

$$\langle f_{Jn} \rangle W_n^{(u)} = \sum_{Jn} \frac{D_{Jn}}{D_u} J_u(J_u+1) W_n^{(u)} = \frac{1}{2} n_u W_n^{(u)}. \quad (11)$$

Then the fractional ENDOR enhancement is optimized when

$$\frac{1}{2} n_u b_u \approx 1. \quad (12)$$

Therefore, the fractional ENDOR enhancement for a proton species with many equivalent protons has a high optimum temperature.

The much smaller value of E_0^{exp} for *t*-butyl protons than for other protons evidently results from the effect of incomplete hf separation. However, the choice of the value of T_{2e} involves ambiguities, because inhomogeneous broadening unfortunately prevents an estimate of T_{2e} from the unsaturated ESR linewidth. The T_{1e} of galvinoxyl in *s*-butylbenzene, determined by Huisjen and Hyde[19] from saturation recovery, has a value in the range of 1—10 μs at −30 °C. If the extreme narrowing condition is satisfied at this temperature, T_{2e} may also be of the same order of magnitude. Here, T_{2e} was taken as a constant with a value of 1.2 μs, from consideration of the behavior of the ESR linewidth mentioned above. Then, the optimization process for *t*-butyl protons gave $b_{tb}=0.13$ at −70 °C, whereas $b_{tb}=1/18$ at −55 °C or $b_{tb}=0.19$ at −70 °C, from Eq. 12. It is felt that these values of b_{tb} are rather large compared with those for other protons. A possible explanation may be the closeness of the location of *t*-butyl protons to oxygen atom which has large spin density, resulting in large END terms. The theoretical solid curves, calculated from Eqs. 49—52 in part I, are close the experimental curves in Figs. 7 and 8. Also, Fig. 9 shows that the ratio of E_0^{exp} for *t*-butyl protons to that for a methylidyne proton decreases monotonically with temperature, in contrast to the ratio for ring protons. Such a feature is again described by the theoretical solid lines. It is to be noted that the dotted line, calculated from Eq. 50 in part I in which the first factor is omitted, has a value much smaller than 36, except at extremely high temperatures. The above discussion should not be taken too seriously since the present lack of information about the internal motion of the *t*-butyl group prevents further considerations, such as of the isotopic hf modulation. Nevertheless, it is felt that the essential features of the ENDOR quotient for *t*-butyl protons can be explained by the effect of incomplete hf separation and the large average multiplicity for this proton discussed above.

In conclusion, it may be said that the theory in part I describes fairly well the ENDOR relaxation of galvinoxyl.

The authors wish to express their gratitude to Professor K. Kuwata of Osaka University for stimulating and helpful discussions throughout the course of this work.

References

1) W. B. Mims, *Rev. Sci. Instrum.*, **36**, 1472 (1965).
2) M. Huisjen and J. S. Hyde, *Rev. Sci. Instrum.*, **45**, 669 (1974).
3) R. G. Kooser, W. V. Volland, and J. H. Freed, *J. Chem. Phys.*, **50**, 5243 (1969).
4) D. S. Leniart, H. D. Connor, and J. H. Freed, *J. Chem. Phys.*, **63**, 165 (1975).
5) J. S. Hyde and A. H. Maki, *J. Chem. Phys.*, **40**, 3117 (1964).
6) R. D. Allendoerfer and A. H. Maki, *J. Magn. Reson.*, **3**, 396 (1970).
7) A. J. Barlow, J. Lamb, and A. J. Matheson, *Proc. R. Soc.*, **292**, 322 (1966).
8) J. H. Freed, D. S. Leniart, and J. S. Hyde, *J. Chem. Phys.*, **47**, 2762 (1967).
9) D. H. Whiffen, *Mol. Phys.*, **10**, 595 (1966).
10) The plot for *t*-butyl protons appears to be curve downward. This fact is explained by the theory in part I for a multi-level system, *i. e.*, a plot of y^{-1} *vs.* x^{-1} in Eq. 53 of part I is, strictly saying, curve downward.
11) Y. Kotake and K. Kuwata, *Bull. Chem. Soc. Jpn.*, **47**, 45 (1974).
12) K. Ishizu, M. Ohnishi, and H. Shikata, *Bull. Chem. Soc. Jpn.*, **50**, 76 (1977).
13) J. H. Freed, D. S. Leniart, and H. D. Connor, *J. Chem. Phys.*, **58**, 3089 (1973).
14) J. H. Freed and G. K. Fraenkel, *J. Chem. Phys.*, **39**, 326 (1963).
15) J. H. Freed, *J. Chem. Phys.*, **43**, 2312 (1965).
16) N. M. Atherton and B. Day, *Mol. Phys.*, **27**, 145 (1974).
17) G. R. Luckhurst, *Mol. Phys.*, **11**, 205 (1966).
18) J. H. Freed, *J. Phys. Chem.*, **71**, 38 (1967).
19) M. Huisjen and J. S. Hyde, *J. Chem. Phys.*, **60**, 1682 (1974).